Detection of EEG dynamic complex patterns in disorders of consciousness

Running head: EEG patterns in disorders of consciousness

Gabriel A. Della Bella MSc,[1,2,†] Di Zang MD. PhD,[3,4,5,6,7,8,†] Peng Gui PhD,[9,†] Diego M. Mateos PhD,[10,11] Jacobo D. Sitt PhD,[12,13] Tristan A. Bekinschtein PhD,[14] Dragana Manasova PhD,[12,15] Benjamine Sarton MSc,[16,17] Fabrice Ferre MSc,[16,17] Stein Silva MD. PhD,[16,17] Pedro W. Lamberti PhD,[2,18] Xuehai Wu MD. PhD,[3,4,5,6,7] Ying Mao MD. PhD,[3,4,5,6,7] Liping Wang PhD,[9*] and Pablo Barttfeld PhD,[1*]

[†]These authors contributed equally to this work. [*]Co-senior authors.

1 Cognitive Science Group. Instituto de Investigaciones Psicológicas (IIPsi,CONICET-UNC), Facultad de Psicología, Universidad Nacional de Córdoba, 5000, Córdoba, Argentina.

2 Facultad de Matemática Astronomía y Física (FaMAF), Universidad Nacional de Córdoba, 5000, Córdoba, Argentina.

3 Department of Neurosurgery, Huashan Hospital, Shanghai Medical College, Fudan University, 200040, Shanghai, China.

4 National Center for Neurological Disorders, 200040, Shanghai, China.

5 Shanghai Key Laboratory of Brain Function and Restoration and Neural Regeneration, 200040, Shanghai, China.

6 Neurosurgical Institute of Fudan University, 200040, Shanghai, China.

7 Shanghai Clinical Medical Center of Neurosurgery, 200040, Shanghai, China.

8 Department of Neurosurgery, China-Japan Friendship Hospital, Beijing, 100029, China

9 Institute of Neuroscience, Key Laboratory of Brain Cognition and Brain-Inspired Intelligence Technology, CAS Center for Excellence in Brain Science and Intelligence Technology, Chinese Academy of Sciences, Shanghai 200031, China.

10 Consejo Nacional de Investigaciones Científicas y Técnicas (CONICET), Buenos Aires, Argentina.

11 Achucarro Basque Center For Neuroscience. Leioa, Vizcaya, Spain.

12 Sorbonne Université, Institut du Cerveau–Paris Brain Institute–ICM, Inserm, CNRS, APHP, Hôpital de la Pitié Salpêtrière, 75013, Paris, France.

13 Inserm U 1127, F-75013 Paris, France.

14 Department of Psychology, University of Cambridge, Cambridge, CB2 3EB, United Kingdom.

15 Université Paris Cité, 75006 Paris, France.

16 Réanimation URM CHU Purpan, Cedex 31300 Toulouse, France.

17 Toulouse NeuroImaging Center INSERM1214, Cedex 31300 Toulouse, France.

18 Institute of Theoretical Physics, Jagiellonian University, ul. Łojasiewicza 11, 30–348 Kraków, Poland.

The corresponding author contact information:

Peng Gui. Institute of Neuroscience, Key Laboratory of Primate Neurobiology, CAS Center for Excellence in Brain Science and Intelligence Technology, Chinese Academy of Sciences, Shanghai 200031, China. pgui@ion.ac.cn

Abstract

A major challenge in cognitive neuroscience is developing reliable diagnostic tools for Disorders of Consciousness (DoC). Detecting dynamic brain connectivity configurations holds great promise for advancing diagnostics. Evidence indicates that certain fMRI-derived connectivity patterns are closely tied to the level of consciousness. However, their clinical utility remains constrained by practical limitations. In this study, we introduce EEG-based brain states as a real-time, bedside tool for detecting periods of enhanced brain activity in DoC patients. We analyzed data from 237 patients with chronic and acute DoC from three different centers and identified five EEG functional connectivity recurrent brain patterns. The occurrence probabilities of these patterns were strongly correlated with patients' levels of consciousness. High-entropy patterns were found exclusively in healthy participants, while low-entropy patterns became more prevalent with increasing DoC severity, crucially predicting individual recovery outcomes. To assess the real-time applicability of this approach, we conducted tests demonstrating reliable, real-time estimation of patient brain patterns, confirming the feasibility of bedside detection. Our findings highlight the potential of EEG for real-time, bedside monitoring of brain dynamical connectivity patterns, significantly deepening our understanding of the neural dynamics underlying consciousness and paving the way for future discoveries in brain state research.

Introduction

Diagnosing disorders of consciousness (DoC) and prognosing patients' evolution remain a major medical challenge. Current classifications of DoC are based primarily on clinical evaluations of arousal and awareness, leading to the categorization of patients into a heterogeneous set of categories with definitions that are still evolving [1,2]. However, these assessments, which rely on overt behavioral responses, are inherently limited and are susceptible to bias from factors affecting motor output (e.g. locked-in syndrome)[3,4] or language function (e.g. aphasia)[5,6]. As a result, diagnostic errors are common, with misdiagnosis rates estimated as high as 40%[7], often leading to critical treatment decisions.

Given these limitations, there is a growing need for objective, neurophysiological markers that can provide a more accurate assessment of consciousness. One promising avenue of research lies in the study of brain signal complexity and information dynamics. In this context, entropy, a measure of the unpredictability or disorder within a system, has emerged as a powerful tool to characterize different states of consciousness, with theoretical and practical implications. Studies in neuroscience have extensively explored the relationship between entropy and consciousness, particularly in the contexts of coma, anesthesia, and sleep[8–10]. Higher entropy has been associated with wakefulness and cognitive flexibility, whereas lower entropy reflects diminished neural complexity, often observed in unconscious states[11,12]. Recent findings indicate that brain entropy systematically decreases in coma, anesthesia, and deep sleep, reflecting a shift toward more predictable and less integrated neural states[8,13]. This pattern is consistent with the loss of long-range functional connectivity and thalamocortical disruptions observed in unconscious states[14]. A set of studies have proposed that consciousness emerges from the brain's dynamic organization, following the MaxCon (Maximization of Configurations) principle[15–17]. This framework suggests that conscious states arise when the brain optimally balances integration and segregation of information, maximizing network complexity. By analyzing entropy and brain connectivity across different states (e.g., anesthesia, coma, wakefulness), the authors provide evidence that consciousness corresponds to maximal configurational diversity and information distribution.

However, entropy-based approaches alone may not fully capture the complexity of conscious states. Sanz Perl et al.[18] demonstrated that macroscopic brain activity deviates from equilibrium during wakefulness, a property that is lost in unconscious states. Using entropy production and the curl of probability flux in phase space, they showed that wakefulness is characterized by persistent non-equilibrium dynamics, whereas unconscious states, including those induced by propofol and ketamine anesthesia, shift toward equilibrium conditions. In active states such as wakefulness, the number of possible system configurations, representing the different ways in which brain regions can connect, is maximized. From the standpoint of statistical physics, this corresponds to a tendency to maximize entropy. In contrast, altered states such as sleep[19], anaesthesia[20], or DoC[21] show a reduction in the number of possible configurations, leading to lower entropy[16]. This perspective aligns with the idea that a rich repertoire of network configurations, rather than just a high level of entropy, is essential for conscious experience. Beyond traditional measures of neural complexity, recent work has framed consciousness as a non-equilibrium phenomenon, highlighting the brain's deviation from thermodynamic equilibrium as a fundamental signature of awareness[18]. Various theories of consciousness have incorporated entropy as a fundamental principle to explain conscious states and their fluctuations. In general, these theories suggest that consciousness emerges from neural dynamics that balance order and disorder, where entropy reflects the brain's ability to process information flexibly and adaptively. From a thermodynamic perspective, the theory of the brain as a non-equilibrium system posits that consciousness arises when the brain operates far from thermodynamic equilibrium, maintaining a stable yet highly variable dynamic[18,22]. According to this view, unconscious states reflect a reduction in neural complexity and a shift toward more predictable, equilibrium-like dynamics. Signal entropy has been widely studied as a correlate of consciousness, with measures derived from EEG time-series (e.g., spectral entropy, Lempel-Ziv complexity) consistently showing reduced complexity in unconscious states. However, these approaches primarily capture local neural signal variability rather than large-scale network coordination. In contrast, connectivity entropy quantifies the diversity of functional interactions across brain regions, offering a complementary perspective on the neural dynamics of consciousness. Together, these theories suggest that consciousness is deeply linked to the regulation of entropy in the brain. While conscious states are characterized by high but structured entropy, unconscious states reflect a

decline in complexity and a shift toward equilibrium-like dynamics. Understanding how entropy interacts with other neural properties remains a key challenge in consciousness research.

Recent advancements in neuroimaging, guided by the aforementioned findings on entropy and complexity, as well as connectionist theories of consciousness[8,23–26], have sought to characterize conscious states by identifying brain activity patterns that may not be detectable through behavioral assessments. These techniques have emerged using active cognitive tasks[21,27–29], spontaneous brain activity[9,30–32], and external stimulation paired with EEG responses[33–35], providing clinicians with new tools to detect consciousness. Among these methods, one of the most promising approaches is based on studying signatures of consciousness through the detection of fMRI-based “brain states"[13,36–39], which is especially well suited to detect spontaneous, transient shifts in brain activity. These brain states refer to recurring patterns of functional connectivity obtained through unsupervised clustering of dynamical connectivity matrices that can reveal these shifts (typically lasting from 5 to 60 seconds[36]). Research indicates that the properties of the brain states are strongly modulated by levels of arousal and consciousness. In awake humans and monkeys a diverse range of brain states exists, including those with high connectivity, high entropy, and negative correlations[13,36,38,39]. Conversely, in cases of DoC or under sedation, there are significant changes in the observed brain states: the richer variety of brain states diminishes, and only low-connectivity, low-entropy states —shaped by the underlying structural connectivity— persist[9,37]. These findings are in line with dynamical systems simulations[40,41] showing that, for low coupling strength between brain areas —a configuration resembling DOC condition—spontaneous neuronal activity remains but it is restricted to a single stable connectivity pattern, defined by the fixed network of structural connectivity. As connectivity between brain regions increases, the system undergoes a transition to multistability, allowing for a diverse set of possible patterns. This transition is considered crucial for sustaining conscious states.

However, the reliance on fMRI for detecting brain states presents significant practical challenges in the clinical management of DoC. Transporting patients with life-supporting devices to MRI scanners is often unfeasible, and repeated scanning over long periods is required to capture the transient periods of heightened brain activity, which is impractical

in a scanner setting. In contrast, EEG offers a more accessible and real-time alternative, allowing bedside assessments that could provide critical insights into patients' residual brain function and consciousness. By leveraging EEG-based brain state detection, we can move toward more personalized patient care, allowing clinicians to monitor transient changes in brain dynamics.

In this study, we analyzed one of the largest cohorts of DoC patients to date, comprising 237 patients and 101 healthy controls from three independent clinical centers, aiming to bring EEG-based consciousness detection closer to clinical application. We expanded upon previous work that focused mainly on chronic DoC, such as Unresponsive Wakefulness Syndrome (UWS) and Minimally Conscious State (MCS), by including both chronic and acute patients. The acute group included comatose individuals with low Glasgow Coma Scale (GCS) scores, with an average of 14 days since brain injury. Our goal was to identify EEG-based brain states and explore their diagnostic and prognostic potential across the full spectrum of DoC. (Fig. 1A). Our findings revealed and characterized five distinct EEG functional connectivity brain states, whose occurrence probability was closely associated with the level of consciousness. High-entropy brain states were predominantly observed in conscious subjects, while low-entropy states became more probable with increasing DoC severity. Moreover, we found that transient patterns of high-entropy connectivity — akin to those seen in healthy individuals — could occasionally be detected in DoC patients. The occurrence probability of these patterns provided valuable diagnostic information and offered predictive insights into patient outcomes. Finally, we demonstrated that these transient states of enhanced connectivity could be detected in real-time using bedside EEG, highlighting the feasibility of this method for continuous patient monitoring and neuroprognostication (Fig. 1).

Results

Methodological overview

The analyses applied in this work are illustrated in Fig. 1. EEG data from three distinct sites were first transformed into symbolic representations using weighted Symbolic Mutual Information (wSMI)[21] (see Supplementary Methods and Fig. S1 for a full description of the process). This measure identifies non-random joint fluctuations between two EEG signals, allowing for the detection of meaningful patterns in brain connectivity. Next, k-means clustering was employed on these wSMI connectivity matrices to identify recurring connectivity patterns across all subjects, referred to as “brain states”[13,37,38] (Fig. 1A). These

196 brain states were then sorted based on the Shannon entropy of the distribution of
197 connectivity values. Each brain state was classified by its proximity to the connectivity
198 matrices, resulting in a probability distribution for each subject (Fig. 1A, right). To
199 summarize the properties of these brain states, we calculated the Weighted Entropy (WE),
200 which represents the average entropy weighted by the probabilities. The WE metric
201 reflects the diversity and complexity of connectivity patterns across brain states, with
202 higher WE values indicating more varied and complex connectivity. To investigate the
203 relationship between these brain states and clinical outcomes, patients were categorized
204 into three groups based on their clinical evolution: *improvement* (e.g., transition from UWS
205 to MCS), *no change* (e.g., staying in the same condition), and *deterioration* (e.g., transition
206 from MCS to UWS).

207 **Detection of EEG brain states**

208 We identified five distinct EEG brain states, with the value of five determined using the
209 Elbow method[42] (Fig. S2; see Supplementary Material for details), each characterized by
210 unique connectivity patterns. To streamline analysis and comparison, we ranked the brain
211 states by entropy levels (Fig. 2A), assigning numbers in descending order. Consistent with
212 previous findings in fMRI studies, brain states 1 and 2 displayed the highest entropy and
213 complexity (Fig. 2D). These states displayed a broad spectrum of connectivity values,
214 ranging from weak to strong connections across electrodes in a topographical map,
215 suggesting the presence of connectivity hubs in parietal regions (Fig. 2A). On the opposite
216 end of the entropy scale, brain states 4 and 5 exhibited a completely different connectivity
217 pattern. These states showed a narrow connectivity range with uniformly low connectivity
218 values, leading to a homogeneous distribution of connections across the scalp (Fig. 2A,
219 right). Using hierarchical decomposition analysis of the brain state space, we observed
220 similarities according to the Manhattan distance and positions between the different brain
221 states (Fig. 2C). Brain states 4 and 5 formed a cluster with the highest similarity, followed
222 by their merging with brain states 3 and 2 (Fig. 2C). Brain state 1 exhibited the greatest
223 distance from the other brain states, indicating its distinctiveness in the multidimensional
224 space.

225 **EEG brain states rates of occurrence across levels of consciousness**

226 Figure 2B depicts the distribution of brain states across different groups based on the
227 severity of DoC. Both the probability of each brain state (Fig. 2B) and the average WE
228 (Fig. 2E) were consistently modulated by the participant's condition. Compared to controls,

the patients' probability of high-entropy brain states diminished (Fig. 2B), the probability of low-entropy states increased, and the average weighted entropy decreased (Fig. 2E). As DoC severity increased from MCS to UWS to Acute, the WE progressively shifted towards lower values in patients compared to controls (Fig. 2E) ($F_{3, 153.1} = 25.45$, $p = 2\times10^{-13}$). Significant differences in WE were observed between the control group and all patient groups (Healthy vs. MCS [(-0.01141 ± 0.00254), t-ratio$(294.8) = -4.497$, $p = 0.0001$], Healthy vs. UWS [(-0.01521 ± 0.00250), t-ratio$(294.9) = -6.081$, $p < 0.0001$], Healthy vs. Acute [(-0.02627 ± 0.00440), t-ratio$(82.1) = -5.967$, $p < 0.0001$]). However, within the patient group, significant differences in WE were found only between MCS and Acute ([(-0.01486 ± 0.00515), t-ratio$(54.1) = -2.883$, $p = 0.028$]).

To ensure the robustness of our findings, we conducted separate analyses for each center, confirming that the observed patterns held across all datasets (Fig. S3A and Supplementary Methods). To further validate our results, we performed a cross-validation approach, using centroids calculated in one center and testing them in another, which confirmed the generalizability of our findings (Fig. S3 B, C). Additionally, these findings remained stable even when reducing the number of EEG channels, as analyses with 64 and 32 channels yielded similar results to those obtained with 128 channels (Fig. S4). This consistency across datasets, channel configurations, and validation methods strengthens the reliability of our results.

Patient-Specific EEG Brain States

To refine our analysis, we re-ran the clustering algorithm, this time excluding data from healthy controls. This approach allowed us to focus exclusively on the portion of the multidimensional space occupied by the patient's data, enabling a more detailed characterization of their EEG brain specific to the patients. To differentiate these newly identified states from those obtained in the full dataset, we refer to them as Patient-Specific Brain States (PBS), labeled as PBS1, PBS2, and so on. For this analysis, we combined data from the Paris and Shanghai datasets while excluding the Toulouse dataset to avoid collinearity issues, as the Toulouse dataset contained only acute patients. By restricting the analysis to the Paris and Shanghai datasets, we were able to perform a mixed model analysis on chronic patients and evaluate the method's potential for both prognosis and diagnosis.

As expected, the newly identified brain states exhibited significantly lower wSMI values and more diffuse topographies (Fig. 3A) and lower levels of LZ complexity and entropy (Fig. 3C). Consistent with our previous findings, the probability of each individual brain state (Fig. 3B), and WE (Fig. 3D) varied across patient groups, indicating that as the severity of DoC increased from MCS to UWS, WE progressively shifted towards lower values (Fig. 3D) ($F_{3, 183.82} = 18.7$, $p = 1.2\times10^{-10}$). Using centroids obtained exclusively from patient data, we observed significant differences between MCS and UWS (95% CI [0.00344, 0.00728], t-ratio(332.1) = 2.793, p = 0.0282).

Prognostic Value of EEG Brain States

Next, we investigated the potential of our methodology in predicting patient prognosis. In chronic patients, we found a significant relationship between patient outcomes and WE ($F_{2, 178.6} = 4.808$, $p = 0.009$; Fig. 4A and Fig. S5). Specifically, patients who showed improvement in their condition (i.e., transitioning from UWS to MCS) had higher WE (including patients who transitioned from MCS to MCS+ in the improvement group did not change the results; however, we excluded them from the analysis as they represented only three cases), while those who experienced deterioration (transitioning from MCS to UWS or dying) had lower WE. Pairwise comparisons adjusted for multiple comparisons revealed significant differences between the Deteriorate and Improve groups (95% CI [0.000759, 0.00740] p = 0.0115). However, no significant differences were observed between the Deteriorate and No change groups (95% CI [-0.00245, 0.00448], p = 0.77) or the No change and Improve groups (95% CI [-0.000156, 0.00628], p = 0.065).

Similarly, in acute patients we found a significant relationship between patient outcomes and WE ($F_{2, 38} = 5.947$, $p = 0.00566$; Fig. 4B). Significant differences were observed between the No change group (patients transitioning to UWS) and the Deceased group (0.0521, 95% CI [0.0085, 0.0958], p = 0.016), as well as between the Improve group (patients transitioning to MCS) and the Deceased group (0.0522, 95% CI [0.0121, 0.0922], p = 0.008). However, no significant differences were found between the Improve and No change groups (5×10^{-5}, 95% CI [-0.039, 0.039], p = 0.99).

Towards Real-Time EEG Monitoring of Patients

To assess the practical potential of this methodology, its performance was tested in a simulated real-time bedside setting. Although real-time data were not available, we

conducted a simulation of real-time assessment on acute patients using our pipeline (see Supplementary Methods for a detailed explanation of the procedure). We classified segments of raw EEG signals into one of the five brain states previously defined for the patients (Fig. 1B). We compared the similarity between offline and real-time brain state distributions in patients, along with their corresponding WE values. Statistical analysis revealed no significant differences in WE values between the two conditions ($F_{1, 78} = 0.713$, $p = 0.401$), indicating that the real-time classification effectively replicated the distribution observed in the offline analysis (Fig. 5A). Figure S5B displays the high degree of similarity between offline and real-time classifications. The average WE values for each patient remained highly stable between the two conditions ($R = 0.98$) (Fig. 5B), suggesting that our methodology can reliably capture patient-specific brain states in a real-time context. We also quantified the similarity between real-time and offline distributions using a bootstrap method (see Supplementary Methods for details). To assess this similarity, we computed the Jensen-Shannon divergence between the distributions (Fig. 5C). The results showed that the divergence between real-time and offline distributions was not significantly different from random fluctuations when classifying real-time data based on the offline brain states of the same acute patients ($p = 0.47$).

We further explored the potential of our simulated real-time method by assessing its ability to predict prognosis, as we previously did in the offline analysis. In acute patients, we found that real-time mean values, obtained from a single real-time recording, could distinguish between patients who improved and those who deteriorated just as effectively as the offline analysis ($F_{2, 38} = 7.47$, $p = 0.001$). We found significant differences in No change vs. Deteriorate (0.05, 95% CI [0.01, 0.09], $p = 0.004$) and Improve vs. Deteriorate (0.05, 95% CI [0.01, 0.08], $p = 0.003$) but no significant difference between in No change vs. Improve (-0.002, CI [-0.03, 0.03], $p = 0.97$). Next, we used the probability values of each brain state as features to train a Logistic Regression classifier to differentiate between the control and acute groups. The model, evaluated using a leave-one-out cross-validation approach, achieved an AUC of 0.80, an accuracy of 0.76, and an F1-score of 0.81. These results demonstrate that the real-time classification framework effectively captures meaningful differences between conditions, highlighting its potential for practical application.

Discussion

In this study, we investigated EEG brain states in healthy individuals and patients with DoC, identifying distinct brain states and demonstrating their relevance to patient categories and recovery probabilities. We also established the feasibility of real-time, bedside brain state detection, offering a reliable estimation of the patient's current brain state.

EEG Brain States and Their Link to Consciousness

Our findings align with previous research on functional connectivity in DoC patients, as the EEG brain states we identified reflect topographical patterns consistent with those seen in prior research on wakefulness and DoC states[13,36,37]. Specifically, brain states 1 and 2 exhibit striking similarities with the topographies from healthy individuals in time-averaged wSMI estimations[28,29]. These topographies indicate a temporal organization characterized by long-range coupling between brain regions, resulting in distinct functional connectivity patterns. Notably, these patterns encompass both low and high magnitude wSMI values and feature a prominent connectivity hub located at bilateral parietal cortices. Conversely, brain states 4 and 5 resemble those observed in fMRI studies conducted on anesthetized monkeys[39,43] and DoC patients[13] using both EEG and fMRI modalities. These patterns are featured by highly distributed and homogeneous low connectivity with diminished or very weak correlation or mutual information.

These results reinforce theories of consciousness emphasizing long-distance connectivity and dynamic interaction between brain regions as critical for the emergence and maintenance of conscious states[24,26]. According to current models of consciousness, rich and dynamic functional interactions, along with a diverse repertoire of connectivity patterns, are considered key aspects of conscious processing. These dynamics rely on a certain level of coupling between brain regions, enabling the integration of segregated neural processes and supporting potential conscious awareness[34,44,45]. Conversely, in conditions such as anesthesia, DoC, or non-rapid eye movement (NREM) sleep, brain regions exhibit decreased coupling and functional connectivity converges into a low connectivity pattern that aligns with the underlying anatomical connections. This state is characterized by spatially homogeneous and weak connectivity, with limited segregation or integration of neural activity. It represents a stable and long-lasting brain state associated with reduced conscious awareness[38,43].

The Role of Entropy in Brain State Classification

An essential consideration in entropy-based assessments of consciousness, such as our approach, is that variability in connectivity, rather than the absolute strength of connections, is the primary factor driving changes in entropy. Our analysis comparing connectivity entropy with local signal entropy revealed that while both measures decrease in unconscious states, local signal entropy showed limited classification power in our dataset (Fig. S6C), suggesting that large-scale functional network diversity is a stronger marker of consciousness than local neural complexity alone. This distinction is crucial when analyzing brain states such as epilepsy and coma. In epilepsy, for instance, neural connections are abnormally strong and highly synchronized, yet this excessive rigidity results in low entropy due to a lack of flexible state transitions. A similar pattern is observed in coma, where patients predominantly remain in state 5, a highly stable neural configuration with minimal variation over time. Despite having wSMI values that may appear comparable to wakefulness in absolute terms, the key difference lies in the lack of fluctuation in these values. This reflects the brain's failure to dynamically adapt and process both internal and external information. Thus, entropy-based approaches should not only consider connection strength but also the capacity of the system to transition between different states, as this flexibility is likely a crucial feature of conscious processing. Another crucial aspect to consider is the role of connection variability in entropy, rather than just the strength of connectivity. Studies using wSMI and similar metrics indicate that high entropy is associated with dynamic, flexible neural connections, not necessarily stronger connections[9]. In conditions such as epilepsy, brain activity is highly synchronized, with strong but rigid connections, leading to a low entropy state despite intense neural activity. This suggests that entropy-based measures should account for connection variability rather than absolute connectivity strength when assessing consciousness. While WE is not a direct measure of complexity, it provides insights into the variability of brain state organization, reflecting both the range of connectivity values and the temporal changes in these patterns. This aligns with previous studies that have used temporal dynamics to understand functional connectivity in the brain[8,46].

Clinical Applications and Real-Time Monitoring

Using EEG brain states, we successfully differentiated healthy participants from patients and discriminated between DoC categories. Moreover, we have shown that applicability of our methods is not reliant on high-density EEG systems. While our approach does not

achieve exceptional classification scores compared to recent multimodal approaches that combine multiple metrics, it offers unique advantages. One advantage of our approach is the ability to detect specific windows of enhanced brain activity in real time. This could improve the classification performance of multivariate models that currently do not account for individual fluctuations over time. By combining current EEG classification methods with the identification of these transient brain states, we may develop a powerful tool for the diagnosis and prognosis of patients. Moreover, these tools could foster more productive interactions between healthcare providers and patients by focusing on moments when the patient exhibits brain states 1 and 2. Furthermore, our findings suggest that even the presence of complex brain states can offer valuable insights into the DoC category and patient outcomes. The real-time detection of EEG brain states presents a novel opportunity for bedside diagnosis and intervention. Although richer brain states are rare in DoC patients, traces of these states can still be identified across all DoC categories. This suggests that patients' brains briefly visit richer connectivity patterns. Detecting these transiently rich brain states could potentially be valuable for identifying windows of momentarily enhanced cognition in patients, which can inform optimal communication and intervention strategies. Interventions during these brief states of altered brain dynamics may lead to sustained exploration of the brain state repertoire and possibly associated behavioral changes. Similar approaches, such as deep brain stimulation, have shown promising results in modulating fMRI brain states in anesthetized monkeys[39], suggesting its potential applicability in DoC patients to drive the brain state towards cognitively rich configurations.

Limitations and Open Questions

We were able to discriminate between different DoC subcategories only after excluding healthy controls from the analysis, due to the variability introduced by healthy individuals. The use of k-means clustering posed limitations, as it partitions data into equally sized clusters, impacting the granularity of our findings. Future research should explore more advanced clustering methods that can adjust cluster sizes dynamically to improve discrimination between patient subcategories.

A significant methodological challenge in using EEG to study brain states is the lack of direct information on specific brain regions, unlike fMRI. EEG signals cannot directly map functional to structural connectivity, although structural connectivity plays a crucial role in

shaping brain states, especially under low vigilance. Our approach addressed this by classifying brain states based on entropy. This allowed us to capture the dynamics of brain states without needing direct structural data. Notably, our entropy-based sorting closely mirrored the anatomical organization observed in fMRI studies, suggesting that EEG could offer a reliable means of characterizing brain state dynamics. Future work should explore how to model these results without relying on structural matrices, potentially developing EEG-based models grounded in functional connectivity backbones.

A key limitation of this study, and of research on brain states in general, is the uncertainty regarding their relationship to subjective experience. Neither our study nor previous works have systematically examined whether the same brain state corresponds to similar cognitive or perceptual experiences. While high-entropy states are predominantly observed in conscious individuals, their occasional presence in DoC patients does not necessarily imply awareness. Likewise, the frequent occurrence of low-entropy states in healthy controls does not indicate unconsciousness during those periods. Understanding the functional significance of these brain states requires further investigation into their cognitive content, ideally incorporating experience sampling alongside neurophysiological monitoring.

A particularly intriguing finding is the persistence of low entropy brain states such as number 5 in healthy controls, which aligns with previous fMRI studies but remains poorly understood. This state could reflect transient microsleep episodes, a common but often overlooked phenomenon in resting-state paradigms. Alternatively, it may not indicate a loss of consciousness but rather effortful information processing, occurring between cognitively demanding tasks while subjects remain vigilant. Without direct experience sampling, it is unclear whether this state corresponds to altered awareness. Future research should aim to distinguish between these possibilities by combining EEG-based connectivity analysis with subjective reports and objective wakefulness measures such as eye-tracking or polysomnography.

More broadly, the classification of brain states is constrained by the assumption that they represent discrete functional configurations with distinct cognitive correlates. One key limitation is the lack of direct association between these states and specific mental content. Neither our study nor previous works have systematically investigated whether the same brain state corresponds to similar subjective experiences, leaving open the

possibility that distinct cognitive or perceptual states could map onto the same connectivity configuration. Additionally, k-means clustering assumes that the identified states are equally distributed and well-separated in the feature space. However, the robustness of our clustering analysis regarding the number of brain states to identify (Fig. S2), and the stability of brain states across resting-state and task conditions (Table S2), highlight both strengths and challenges in defining brain states. On one hand, the consistency of results across different clustering solutions and experimental conditions suggests that these findings are not an artifact of arbitrary parameters. On the other hand, this same robustness raises fundamental questions about what constitutes a "brain state"—if states remain unchanged across cognitive conditions, does this imply they are purely structural in nature, or do they reflect intrinsic, flexible neural dynamics that transcend task engagement? To advance our understanding of this topic, future research should integrate experience sampling methods with neuroimaging clustering approaches. This combined strategy would allow us to assess whether fluctuations in brain connectivity correspond to variations in conscious experience, shedding light on the functional significance of these brain states and their role in shaping cognition and awareness.

Our findings also align with in-silico theoretical models[47,48]. From a neural dynamics perspective, high-entropy states may reflect a system operating in a metastable regime, allowing for flexible transitions between functional connectivity configurations, a characteristic often associated with wakefulness and cognitive engagement[45,49]. In contrast, low-entropy states may indicate a system trapped in a more rigid, structurally constrained configuration, which is commonly observed in unconscious states such as deep sleep, anesthesia, and DoC. Notably, the presence of transient high-entropy states in DoC patients suggests that residual network flexibility is preserved to some extent, potentially reflecting brief windows of increased neural complexity that could be relevant for recovery[45]. The prevalence of low-entropy states in healthy controls further underscores that entropy alone is not a direct measure of consciousness but rather one aspect of a broader dynamical framework. Future research should explore how interventions targeting neural network dynamics, such as non-invasive brain stimulation or pharmacological modulation, might influence the stability and transition probabilities of these states, with potential implications for prognosis and therapeutic strategies in DoC.

Conclusion

This study highlights a strong relationship between EEG brain state properties and levels of consciousness. High-entropy brain states are predominantly observed in conscious individuals, while low-entropy states are more prevalent in patients with severe DoC. The occurrence probabilities of these brain states offer crucial insights into patient prognosis. Moreover, we have demonstrated that transient, enhanced connectivity states can be reliably detected in real-time, paving the way for novel diagnostic and therapeutic interventions in DoC patients. By leveraging EEG as a non-invasive, bedside tool, our research contributes to the growing field of digital medicine, enabling continuous, real-time monitoring of brain function. This approach not only deepens our understanding of the neural mechanisms underlying consciousness but also holds the potential to revolutionize clinical workflows with advanced, data-driven diagnostic tools that could transform the care of DoC patients.

Methods

Ethics statement

All data collections have been approved by their respective ethical committees. The Shanghai study was approved by the Ethical Committee of the Huashan Hospital of Fudan University (approval number: HIRB-2014-281). The Paris study was approved by the Ethical Committee of the Pitié Salpêtrière under the French label of '*Recherche en soins courants*' [routine care research]. The Toulouse study was approved by the ethics committee of the University Hospital of Toulouse, Toulouse, France (approval number: RC 31/20/0441). All data collections and analyses were carried out in accordance with the Declaration of Helsinki.

Participants, Recordings and Preprocessing

EEG data were collected from a total of 237 patients and 101 control subjects across three independent datasets (Shanghai, Paris, and Toulouse), resulting in 267 patient recordings and 101 control recordings (see Table S1 for the demographic information). The Shanghai and Paris datasets included chronic patients diagnosed with Minimally Conscious State (MCS) or Unresponsive Wakefulness Syndrome (UWS), while the Toulouse dataset focused on acute patients (see Table S3 for a description of datasets). EEG signals were recorded using Electrical Geodesics systems with high-density electrode nets (HCGSN 257-channel for Shanghai and 128-channel for Paris and Toulouse). Sampling rates

varied across datasets (1000 Hz in Shanghai, 250 Hz in Paris and Toulouse); therefore, the Shanghai data were downsampled to 250 Hz for consistency. Additionally, all datasets were band-pass filtered between 1–40 Hz to ensure spectral uniformity. To facilitate cross-center comparisons, we interpolated the Shanghai and Paris datasets to match a common 128-channel electrode configuration using spherical interpolation (*see Supplementary Methods for details*). Preprocessing pipelines followed standard artifact rejection procedures. Clinical assessments were performed using the Coma Recovery Scale-Revised (CRS-R), and only EEG recordings from patients off sedation for at least 24 hours were included.

Dynamic wSMI calculation

wSMI was used to assess non-random joint fluctuations between EEG signals across electrode pairs. A detailed description of the procedure is provided in the Supplementary Methods. Briefly, EEG signals were transformed into symbolic representations using ordinal patterns with an embedding dimension of d = 3 (resulting in six possible symbols) and a temporal separation of τ = 8 ms, optimizing sensitivity to a broad frequency range. Mutual information was computed using a modified approach that accounts for symbol similarity, reducing spurious correlations from common EEG sources. A Current Source Density transformation (spherical spline surface Laplacian) was applied before computing wSMI. To capture temporal dynamics, EEG sessions were segmented into overlapping 16-second windows with a 1-second shift, balancing sensitivity to brain state transitions while maintaining robust statistical estimation. Connectivity matrices (128×128) were derived for each window and subject. The number of windows varied across datasets due to differences in recording durations, ranging from approximately 8 minutes per subject in the Shanghai dataset to 31 minutes in the Toulouse dataset. All analyses were implemented in Python using NICE Tools, MNE, and scikit-learn [50].

Unsupervised clustering of connectivity matrices

We applied *k*-means clustering to identify recurring connectivity patterns, a method widely used in fMRI research [13,37]. To optimize computational efficiency and ensure equal representation of all EEG recordings, we downsampled each subject's data to 300 windows, distributing selections evenly across the session to avoid temporal biases (*see Supplementary Methods*). For clustering, we used the Manhattan distance as the similarity metric and determined the optimal number of clusters (k = 5) using the Elbow method (Fig.

S2). To account for the deterministic nature of *k*-means, we performed 10,000 replicates with randomized centroid initialization to prevent convergence to local minima. Once the centroids were established, all original connectivity matrices were assigned to the closest brain state based on Manhattan distance. Additionally, we computed topographical plots for each centroid by averaging column values across rows in the centroid matrices to obtain a single value per electrode. This analysis was conducted on two datasets: one including all participants (brain states 1–5) and another including only chronic patients (patient-specific brain states PBS1–PBS5), resulting in two distinct sets of brain states.

Brain state complexity and distribution across DoC

The brain states obtained by k-means clustering were sorted in descending order based on their entropy. To achieve this, we calculated the entropy of the distribution of wSMI values for each centroid by dividing the values into $\sqrt{N}$ bins where N = 128*(128-1)/2 is the number of independent values of the matrix. Additionally, we calculated the Lempel-Ziv complexity (LZC) for each centroid, which quantifies the irreducible information present in a sequence (see Supplementary material for details). The probability of occurrence for each brain state was estimated by determining the proportion of times each individual connectivity matrix was classified as belonging to that specific brain state. This probability was estimated based on all available recording windows, not just the 300 windows selected for clustering.

To quantify the shift of brain state distributions towards specific brain states, we introduced a weighted entropy (WE) defined as follows:

$$WE = \sum_{i=1}^{5} p_i H_i \quad (1)$$

Where p_i is the probability of each brain state and H_i is its entropy.

Instead of relying solely on the probability distribution of k-means centroids, we calculated the entropy of each centroid's connectivity values, which reflects the variability within each pattern. This approach recognizes that even if different centroids have the same probability, their varying entropies will result in different combinations or averages, capturing the underlying complexity of brain states more accurately.

Instead of relying solely on the probability distribution of k-means centroids, we calculated the entropy of each centroid's connectivity values, reflecting the variability within each

pattern. This approach accounts for the fact that some centroids represent more homogeneous and stable connectivity states (lower entropy), while others capture more heterogeneous or rich configurations (higher entropy). Additionally, WE offers a more robust means of comparison across groups, as it ensures that differences in brain dynamics are not solely attributed to frequency shifts but also to changes in the underlying informational structure.

Patients' Outcome

We conducted an analysis of the patients' evolution to examine how brain states might provide information regarding their prognosis. For chronic patients, we defined the potential outcomes as improvement in their clinical condition (e.g., UWS patients transitioning to MCS), deterioration (e.g., patients dying or transitioning from MCS to UWS), or no change in their clinical condition. Similarly, for acute patients, the outcomes were determined based on their progression from an acute condition to a chronic condition, including evolution to MCS, evolution to UWS, or death. A summary of the outcomes since recording can be found in Table S1. Patients for whom the outcome was unknown were denoted as "N/A", and their data were excluded from the prognosis analysis.

Real-time simulation

As a proof of concept, we conducted a real-time simulation to assess the feasibility of EEG brain state classification in acute patients. EEG segments were processed at regular intervals, and their functional connectivity patterns were compared to pre-defined offline brain states. We evaluated the consistency between real-time and offline classifications, confirming that the real-time approach reliably captured brain state distributions. These findings support the potential for bedside, real-time monitoring of brain states in disorders of consciousness. Full methodological details are provided in the Supplementary Materials.

Statistical analysis

Group differences were assessed using mixed linear models to evaluate the relationship between WE and levels of consciousness across different patient groups. Specifically, WE was modeled as a function of group category (Healthy, MCS, UWS, and Acute), with dataset center (Shanghai, Paris, and Toulouse) included as a random effect. Multiple comparison corrections were applied to account for differences across conditions, ensuring statistical robustness. In addition, a separate ANOVA was conducted to assess differences within each dataset, followed by post-hoc Tukey HSD tests to determine pairwise significance.

To examine the prognostic value of EEG brain states, we analyzed the relationship between WE and patient outcomes in both chronic and acute groups. For chronic patients, a mixed linear model was used to assess whether WE varied across patients who improved, remained stable, or deteriorated. For acute patients, where data were available only from a single center, we performed an ANOVA to compare outcome groups. These analyses allowed us to determine whether specific EEG connectivity patterns were predictive of recovery trajectories in disorders of consciousness.

To validate the real-time classification approach, we compared real-time and offline brain state distributions using a bootstrap method and Jensen-Shannon distance analysis. This approach quantified the divergence between the two classification methods, ensuring that real-time EEG monitoring reliably captured the same brain state probabilities as offline analyses. We repeated this comparison across multiple random groupings of patients, demonstrating the robustness of the real-time approach. Full statistical details, model specifications, and additional validation steps are provided in the Supplementary Materials.

Data availability

The data that support the findings of this study are not openly available due to reasons of sensitivity and are available from the corresponding author upon reasonable request.

Code availability

All data was processed using custom MatLab, R and Python software, using specific libraries. Codes are available at https://github.com/dellabellagabriel/doc-brain-states.

Acknowledgments

This research was supported by Agencia Nacional de Promoción Científica y Tecnológica, Argentina (Grants #2018-03614, CAT-I-00083) and Stic Amsud project (CONN-COMA, 2023). GDB and PB were supported by the National Scientific and Technical Research Council (CONICET - Argentina). DZ was supported by Beijing Natural Science Foundation (7254417) and by National High Level Hospital Clinical Research Funding. PG was supported by the National Natural Science Foundation of China (82201352) and the Youth Innovation Promotion Association of Chinese Academy of Sciences (2022267). LW was supported by the CAS Project for Young Scientists in Basic Research (YSBR-071) and the Shanghai Municipal Science and Technology Major Project (2021SHZDZX). YM and XW were funded by the Shanghai Municipal Science and Technology Major Project ([2018SHZDZX01)], ZJLab and the Shanghai Center for Brain Science and Brain-Inspired Technology. XW was also funded by the National Natural Science Foundation of China (82271224). LW is a SANS (Shanghai Academy of Natural Sciences) Exploration Scholar.

We thank Rodrigo Echeveste, Srivas Chennu, Damian Cruse, Demian Engemann, Federico Raimondo and Anat Arzi for useful discussions, and anonymous reviewers for useful suggestions.

Contributions

GADB conceived the project, conceived the analyses, coded and run the analysis, discussed results, wrote the manuscript; DZ conceived the project, designed the experiments and collected the data, conceived the analyses, discussed results, wrote the manuscript; PG conceived the project, designed the experiments and collected the data, conceived the analyses, discussed results, wrote the manuscript; DMM supervised data analysis, wrote the manuscript; JDS, provided data, discussed results, wrote the manuscript; TAB, discussed project and results, wrote the manuscript; DM, collected and provided, wrote the manuscript; BS, collected and provided, wrote the manuscript; FF, collected and provided data, wrote the manuscript; SS, conceived the project, provided data, discussed results, wrote the manuscript; PWL contributed to the implementation of the research, discussed analysis and results, wrote the manuscript; XW contributed to the implementation of the research, wrote the manuscript; YM contributed to the

implementation of the research, wrote the manuscript; LW conceived the project, conceived the analyses, discussed data analysis and results; wrote the manuscript; PB conceived the project, conceived the analyses, discussed data analysis and results; wrote the manuscript.

Conflicts of Interest

There are no conflicts of interest

Abbreviations

CRS-R = Coma Recovery Scale Revised; DoC = Disorders of Consciousness; GCS = Glasgow Coma Scale; LZC = Lempel Ziv Complexity; MCS = Minimally Conscious State; UWS = Unresponsive Wakefulness Syndrome; wSMI = weighted Symbolic Mutual Information; WE = Weighted Entropy; TBI = Traumatic Brain Injury; SAH = Subarachnoid Hemorrhage

References

1. Edlow, B. L., Claassen, J., Schiff, N. D. & Greer, D. M. Recovery from disorders of consciousness: mechanisms, prognosis and emerging therapies. *Nat. Rev. Neurol.* **17**, 135–156 (2021).
2. Naccache, L. Minimally conscious state or cortically mediated state? *Brain* **141**, 949–960 (2018).
3. Formisano, R., D'Ippolito, M. & Catani, S. Functional locked-in syndrome as recovery phase of vegetative state. *Brain Inj.* **27**, 1332–1332 (2013).
4. Laureys, S., Owen, A. M. & Schiff, N. D. Brain function in coma, vegetative state, and related disorders. *Lancet Neurol.* **3**, 537–546 (2004).
5. Majerus, S., Bruno, M.-A., Schnakers, C., Giacino, J. T. & Laureys, S. The problem of aphasia in the assessment of consciousness in brain-damaged patients. *Prog. Brain Res.* **177**, 49–61 (2009).

6. Pincherle, A. *et al.* Early discrimination of cognitive motor dissociation from disorders of consciousness: pitfalls and clues. *J. Neurol.* **268**, 178–188 (2021).
7. Schnakers, C. *et al.* Diagnostic accuracy of the vegetative and minimally conscious state: Clinical consensus versus standardized neurobehavioral assessment. *BMC Neurol.* **9**, 35 (2009).
8. Casali, A. G. *et al.* A Theoretically Based Index of Consciousness Independent of Sensory Processing and Behavior. *Sci. Transl. Med.* **5**, 198ra105-198ra105 (2013).
9. Sitt, J. D. *et al.* Large scale screening of neural signatures of consciousness in patients in a vegetative or minimally conscious state. *Brain* **137**, 2258–2270 (2014).
10. Tagliazucchi, E., Behrens, M. & Laufs, H. Sleep Neuroimaging and Models of Consciousness. *Front. Psychol.* **4**, (2013).
11. Tononi, G., Sporns, O. & Edelman, G. M. A measure for brain complexity: relating functional segregation and integration in the nervous system. *Proc. Natl. Acad. Sci.* **91**, 5033–5037 (1994).
12. Carhart-Harris, R. *et al.* The entropic brain: a theory of conscious states informed by neuroimaging research with psychedelic drugs. *Front. Hum. Neurosci.* **8**, (2014).
13. Demertzi, A. *et al.* Human consciousness is supported by dynamic complex patterns of brain signal coordination. *Sci. Adv.* **5**, eaat7603 (2019).
14. Boly, M. *et al.* Brain connectivity in disorders of consciousness. *Brain Connect.* **2**, 1–10 (2012).
15. Perez Velazquez, J. L., Mateos, D. M., Guevara, R. & Wennberg, R. Unifying biophysical consciousness theories with MaxCon: maximizing configurations of brain connectivity. *Front. Syst. Neurosci.* **18**, (2024).
16. Mateos, D. M., Erra, R. G., Wennberg, R. & Velazquez, J. L. P. Measures of Entropy and

Complexity in altered states of consciousness. Preprint at https://doi.org/10.48550/arXiv.1701.07061 (2017).

17. Guevara Erra, R., Mateos, D. M., Wennberg, R. & Perez Velazquez, J. L. Statistical mechanics of consciousness: Maximization of information content of network is associated with conscious awareness. *Phys. Rev. E* **94**, 052402 (2016).
18. Perl, Y. S. *et al.* Non-equilibrium brain dynamics as a signature of consciousness. *Phys. Rev. E* **104**, 014411 (2021).
19. Miskovic, V., MacDonald, K. J., Rhodes, L. J. & Cote, K. A. Changes in EEG multiscale entropy and power-law frequency scaling during the human sleep cycle. *Hum. Brain Mapp.* **40**, 538–551 (2019).
20. Olofsen, E., Sleigh, J. W. & Dahan, A. Permutation entropy of the electroencephalogram: a measure of anaesthetic drug effect. *Br. J. Anaesth.* **101**, 810–821 (2008).
21. King, J.-R. *et al.* Information Sharing in the Brain Indexes Consciousness in Noncommunicative Patients. *Curr. Biol.* **23**, 1914–1919 (2013).
22. Friston, K. J., Stephan, K. E., Montague, R. & Dolan, R. J. Computational psychiatry: the brain as a phantastic organ. *Lancet Psychiatry* **1**, 148–158 (2014).
23. Dehaene, S., Lau, H. & Kouider, S. What is consciousness, and could machines have it? *Science* **358**, 486–492 (2017).
24. Dehaene, S. & Changeux, J.-P. Experimental and Theoretical Approaches to Conscious Processing. *Neuron* **70**, 200–227 (2011).
25. Mashour, G. A., Roelfsema, P., Changeux, J.-P. & Dehaene, S. Conscious Processing and the Global Neuronal Workspace Hypothesis. *Neuron* **105**, 776–798 (2020).
26. Tononi, G., Boly, M., Massimini, M. & Koch, C. Integrated information theory: from consciousness to its physical substrate. *Nat. Rev. Neurosci.* **17**, 450–461 (2016).

27. Bekinschtein, T. A. *et al.* Neural signature of the conscious processing of auditory regularities. *Proc. Natl. Acad. Sci.* **106**, 1672–1677 (2009).
28. Faugeras, F. *et al.* Probing consciousness with event-related potentials in the vegetative state. *Neurology* **77**, 264–268 (2011).
29. Owen, A. M. *et al.* Detecting awareness in the vegetative state. *Science* **313**, 1402 (2006).
30. Demertzi, A. *et al.* Intrinsic functional connectivity differentiates minimally conscious from unresponsive patients. *Brain J. Neurol.* **138**, 2619–2631 (2015).
31. Malagurski, B. *et al.* Topological disintegration of resting state functional connectomes in coma. *NeuroImage* **195**, 354–361 (2019).
32. Silva, S. *et al.* Disruption of posteromedial large-scale neural communication predicts recovery from coma. *Neurology* **85**, 2036–2044 (2015).
33. Massimini, M. Breakdown of Cortical Effective Connectivity During Sleep. *Science* **309**, 2228–2232 (2005).
34. Stender, J. *et al.* Diagnostic precision of PET imaging and functional MRI in disorders of consciousness: a clinical validation study. *Lancet Lond. Engl.* **384**, 514–522 (2014).
35. Ferrarelli, F. *et al.* Breakdown in cortical effective connectivity during midazolam-induced loss of consciousness. *Proc. Natl. Acad. Sci.* **107**, 2681–2686 (2010).
36. Rosanova, M. *et al.* Recovery of cortical effective connectivity and recovery of consciousness in vegetative patients. *Brain J. Neurol.* **135**, 1308–1320 (2012).
37. Allen, E. A. *et al.* Tracking Whole-Brain Connectivity Dynamics in the Resting State. *Cereb. Cortex N. Y. NY* **24**, 663–676 (2014).
38. Barttfeld, P. *et al.* Signature of consciousness in the dynamics of resting-state brain activity. *Proc. Natl. Acad. Sci.* **112**, 887–892 (2015).
39. Tasserie, J. *et al.* Deep brain stimulation of the thalamus restores signatures of

761 consciousness in a nonhuman primate model. *Sci. Adv.* **8**, eabl5547 (2022).
762 40. Deco, G. *et al.* Awakening: Predicting external stimulation to force transitions between
763 different brain states. *Proc. Natl. Acad. Sci.* **116**, 18088–18097 (2019).
764 41. Kringelbach, M. L. & Deco, G. Brain States and Transitions: Insights from Computational
765 Neuroscience. *Cell Rep.* **32**, 108128 (2020).
766 42. Kodinariya, T. & Makwana, P. Review on Determining of Cluster in K-means Clustering. *Int. J.*
767 *Adv. Res. Comput. Sci. Manag. Stud.* **1**, 90–95 (2013).
768 43. Uhrig, L. *et al.* Resting-state Dynamics as a Cortical Signature of Anesthesia in Monkeys.
769 *Anesthesiology* **129**, 942–958 (2018).
770 44. Giacino, J. T., Fins, J. J., Laureys, S. & Schiff, N. D. Disorders of consciousness after acquired
771 brain injury: the state of the science. *Nat. Rev. Neurol.* **10**, 99–114 (2014).
772 45. Sanz Perl, Y. *et al.* Perturbations in dynamical models of whole-brain activity dissociate
773 between the level and stability of consciousness. *PLOS Comput. Biol.* **17**, e1009139 (2021).
774 46. Luppi, A. I. *et al.* Consciousness-specific dynamic interactions of brain integration and
775 functional diversity. *Nat. Commun.* **10**, 4616 (2019).
776 47. Deco, G., Vidaurre, D. & Kringelbach, M. L. Revisiting the global workspace orchestrating the
777 hierarchical organization of the human brain. *Nat. Hum. Behav.* **5**, 497–511 (2021).
778 48. Kringelbach, M. L. *et al.* Dynamic coupling of whole-brain neuronal and neurotransmitter
779 systems. *Proc. Natl. Acad. Sci.* **117**, 9566–9576 (2020).
780 49. Tagliazucchi, E. & Laufs, H. Decoding Wakefulness Levels from Typical fMRI Resting-State
781 Data Reveals Reliable Drifts between Wakefulness and Sleep. *Neuron* **82**, 695–708 (2014).
782 50. Pedregosa, F. *et al.* Scikit-learn: Machine Learning in Python. *J Mach Learn Res* **12**, 2825–
783 2830 (2011).

Figures and Tables

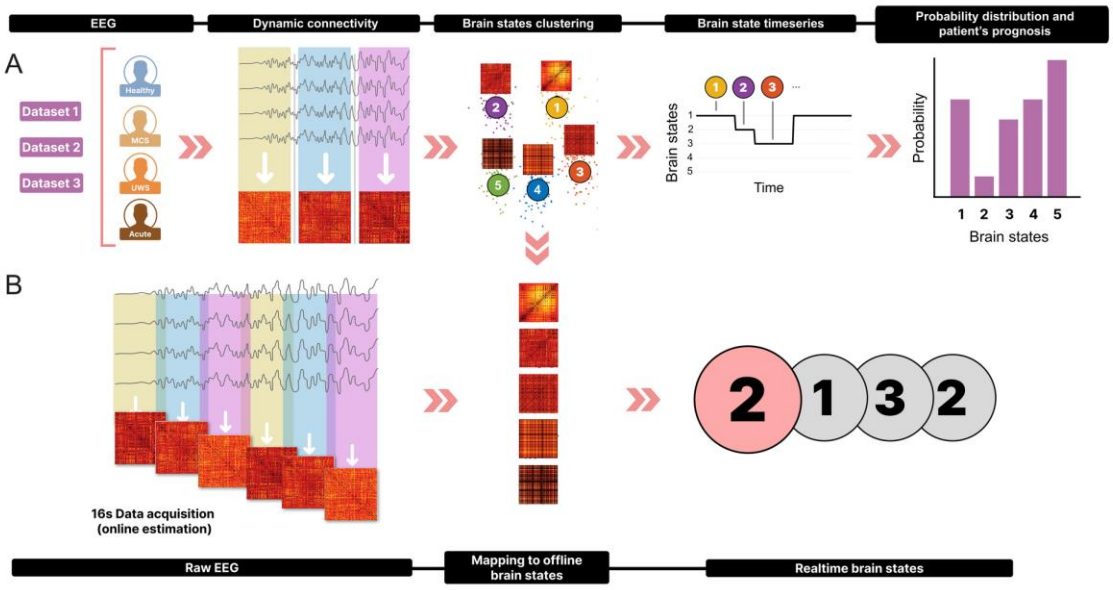

Figure 1. Analysis pipeline. A) Offline calculation of brain states: We utilized three datasets from different centers, comprising healthy controls and three patient categories (Minimally Conscious Syndrome [MCS], Unresponsive Wakefulness Syndrome[UWS], and Acute patients). Windowed wSMI matrices were computed from EEG data, followed by clustering analysis to identify 5 distinct brain states. The probability and association with patient prognosis were then evaluated. B) Real-time calculation of brain states: Simulating a bedside scenario, we processed 16 seconds of raw EEG data every 24 seconds to generate raw-data wSMI matrices. By matching these matrices to the pre-defined brain states obtained offline, we established real-time brain state identification.

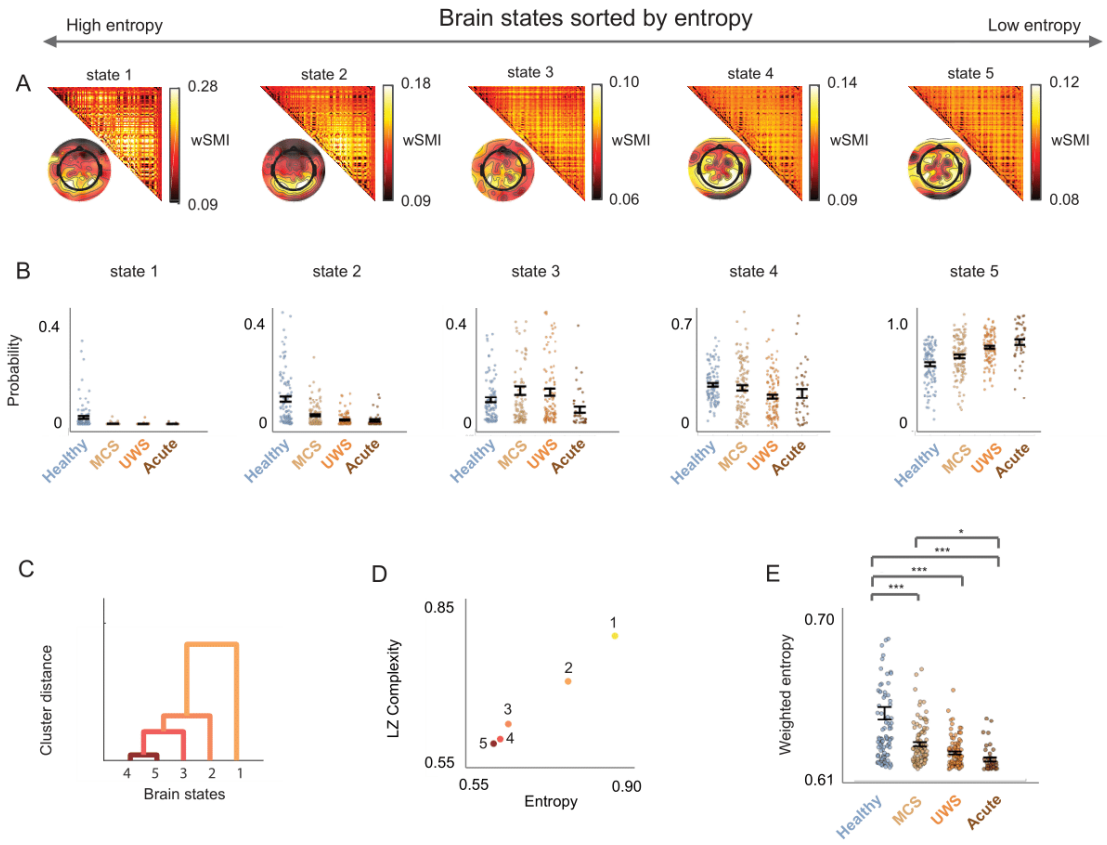

797

798 **Figure 2. EEG brain states and their distribution in DoC.** A) Brain states ordered by
799 entropy from 1 (high entropy) to 5 (low entropy). The upper triangular part of the matrices
800 represents the centroids, or brain states, obtained from the clustering analysis. The value
801 at row *i* and column *j* indicates the wSMI connectivity between electrode *i* and electrode *j*.
802 The topographical plots illustrate the average of wSMI values for each electrode. B)
803 Probability distributions of brain states across all groups. Brain state 1 is predominantly
804 observed in healthy subjects, whereas the probability of brain state 5 increases with the
805 severity of DoC. C) Dendrogram clustering displaying the Manhattan distances between
806 brain states. D) Lempel-Ziv complexity as a function of entropy for each brain state. Brain
807 States with higher variance exhibit greater entropy and Lempel-Ziv complexity. E)
808 Weighted entropy across all groups, highlighting changes in entropy as a function of DoC
809 severity (p-values corrected for multiple comparisons. *p < 0.05, ***p < 0.001).

810

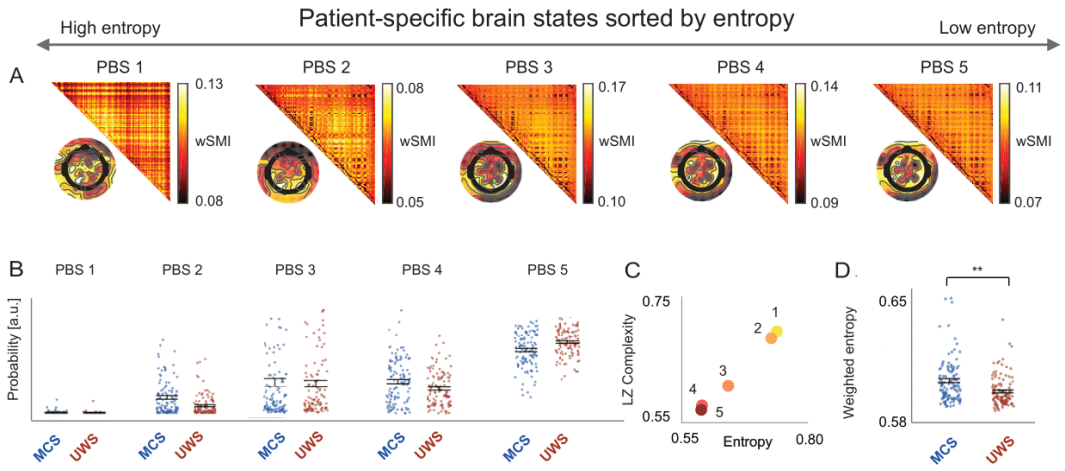

811

812 **Figure 3. Patient-specific brain states. A)** Brain states defined using data exclusively
813 from chronic patients. The upper triangular part of the matrices correspond to the
814 centroids, a.k.a brain states resulting from the clustering analysis, and the value at row i
815 and column j represents the wSMI connectivity value between electrode i and electrode j
816 with brain states sorted by entropy from 1 (high entropy) to 5 (low entropy). The
817 topographical plots show the average wSMI value for each electrode. B) Probability
818 distribution of all 5 brain states for MCS and UWS. C) Lempel-Ziv complexity as a function
819 of entropy for each patient-specific brain state. D) WE for both groups. The weighted
820 entropy values follow the same trend, supporting the differentiation of brain states based
821 on the level of consciousness. (p-values were corrected for multiple comparisons, **p <
822 0.01).

823

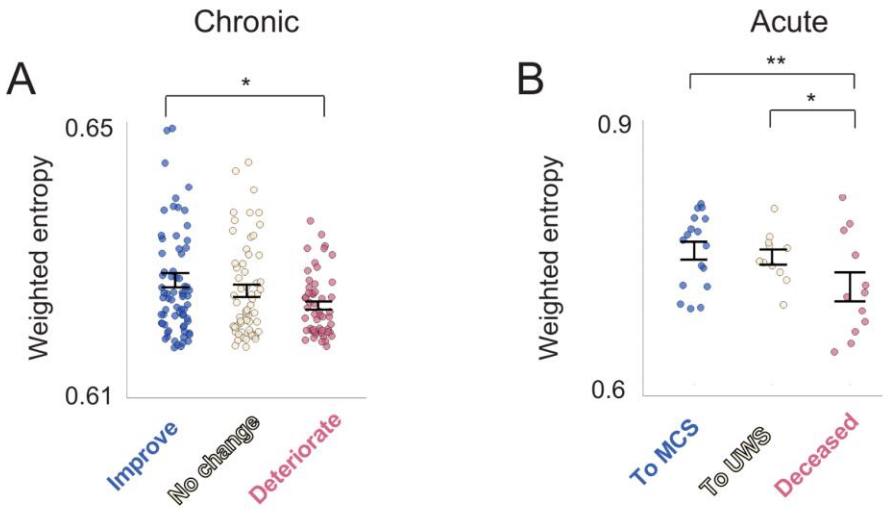

824

825 **Figure 4. Relationship between brain states and patients' prognosis.** A) WE as a
826 function of chronic patients' outcome. The graph shows that in chronic patients, the WE
827 tends to be higher as the probability of patient improvement increases. B) WE as a function
828 of acute patients' outcomes. Similarly, in acute patients, the WE tends to be higher in
829 patients who show improvement in their condition. (p-values were corrected for multiple
830 comparisons, *$p < 0.05$, **$p < 0.01$).

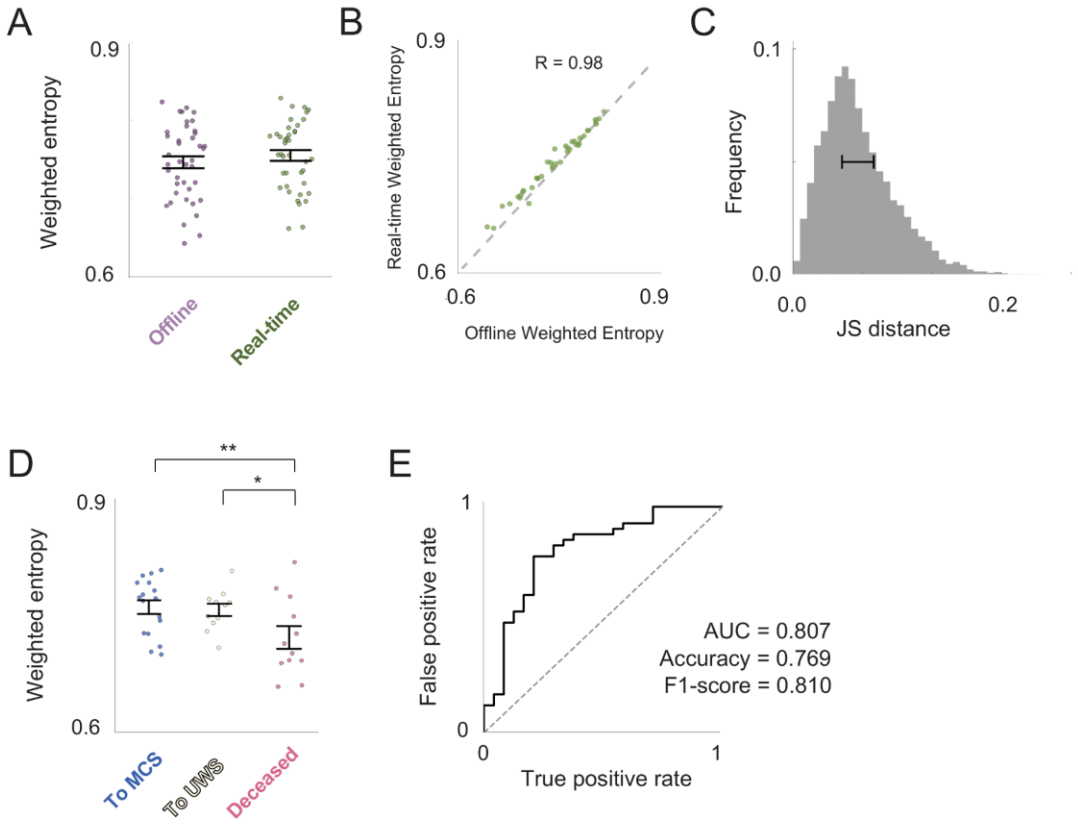

Figure 5. Real-time EEG brain states. A) WE values calculated for acute patients, using both offline and real-time methods. B) Individual WE values calculated in real-time closely matched those obtained through the offline procedure, which included EEG signal cleaning and proper preprocessing. C) The null distribution of Jensen-Shannon distance values between random partitions of the offline data is shown. The error bar represents the estimated value and uncertainty for the real-time calculations, which fall within the distribution, demonstrating the reliability of real-time WE estimation. D) Prognosis as a function of WE values calculated in real-time. E) Classification of patients versus controls based on real-time data. (p-values were corrected for multiple comparisons, *p < 0.05, **p < 0.01).

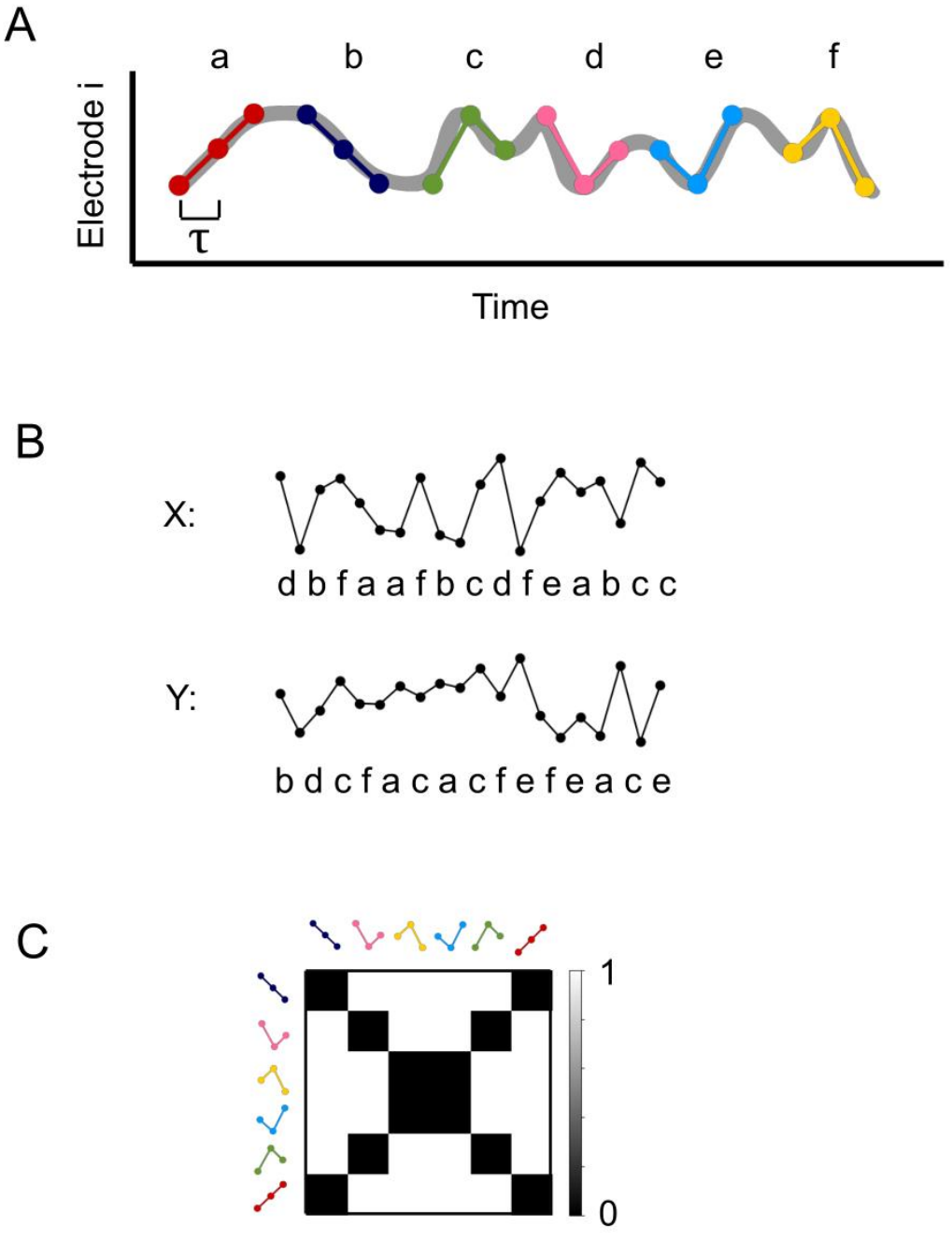

844

845 **Supplementary Figure 1. Schematic of the Weighted Symbolic Mutual Information**
846 **Calculation.** A) The continuous EEG time series from each electrode is transformed into
847 a discrete sequence of symbols. Each symbol consists of three elements, with each

sample separated by a time delay (τ), resulting in a total of six possible symbols based on the signal pattern. B) Once the signal is transformed into its discrete version, a time series of symbols is obtained for each electrode. This allows for the computation of the joint probability distribution between electrodes X and Y, enabling the calculation of Symbolic Mutual Information. C) To prevent contamination from passive cranial conductivity artifacts, and in accordance with methodological references, the mutual information matrix is weighted by disregarding equal and opposite symbols. Additionally, diagonal elements, representing mutual information calculations between identical channels, are removed to ensure that only non-identical symbols contribute to the final wSMI measure.

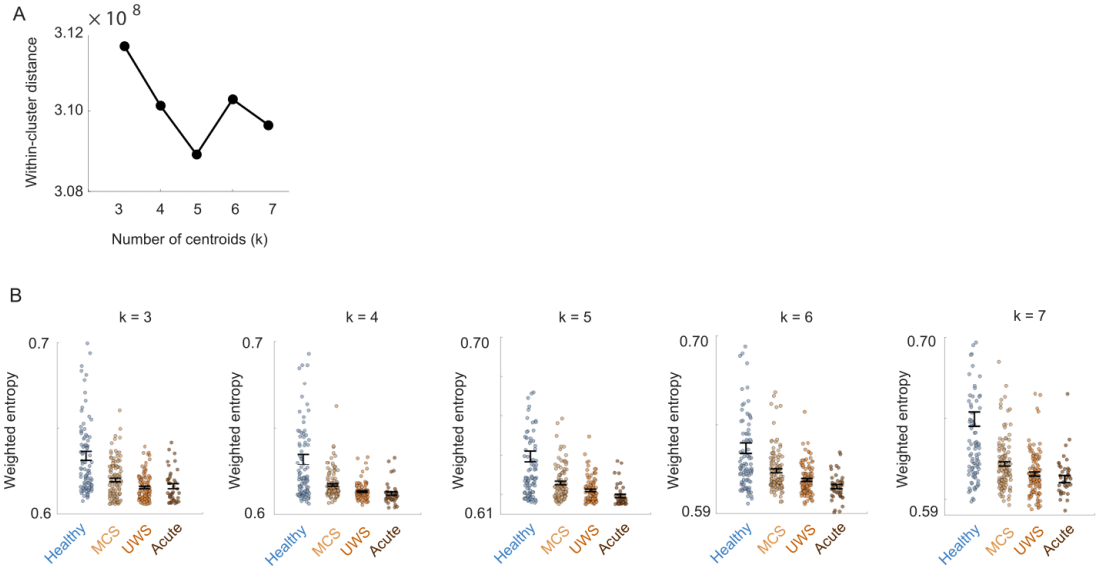

Supplementary Figure 2. Optimal Number of Clusters. A) Within-cluster distance as a function of the number of clusters (k) for k = 3 to 7. The within-cluster distance reaches its minimum at k = 5 (the "elbow"), indicating that this is the optimal number of clusters that balance compactness and interpretability. B) WE across conditions for k = 3 to k = 7. Regardless of the number of centroids considered, WE decreases monotonically from Healthy to Acute, demonstrating a robust trend across clustering solutions.

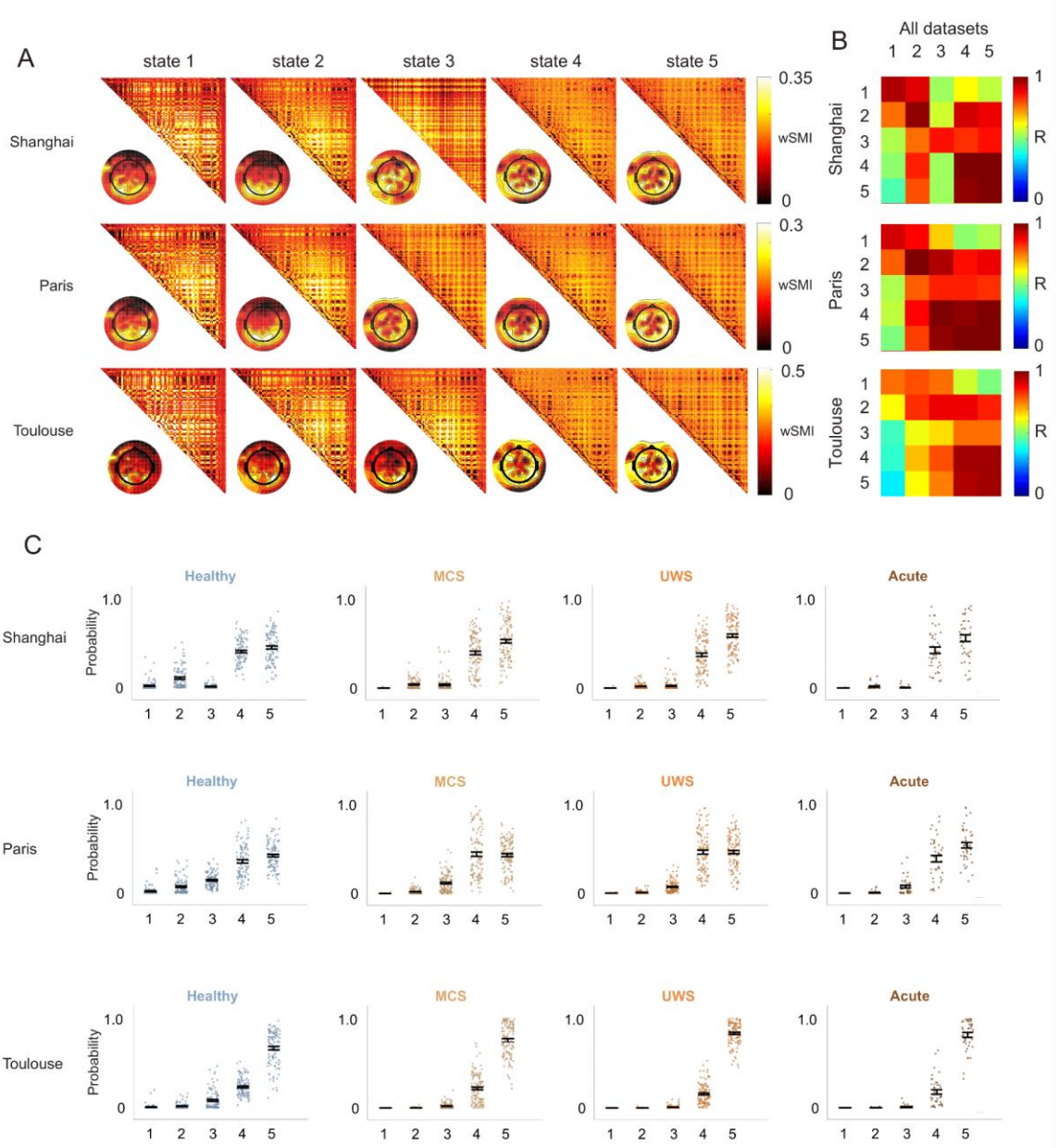

865

866 **Supplementary Figure 3. Cross-Site Brain State Correlations.** A) Brain states
867 identified through clustering analysis applied separately to each site. The matrices
868 represent the wSMI connectivity patterns corresponding to each brain state. The
869 accompanying topoplot is derived by averaging the columns of the matrices, providing a
870 visualization of the average connectivity per electrode. B) Correlation analysis between
871 centroid *i* from the combined dataset across all sites and centroid *j* from each individual
872 site, assessing the consistency of brain state representations across different recording

locations. C) Probability distribution across conditions using brain states obtained from Shanghai (top), Paris (middle) and Toulouse (bottom).

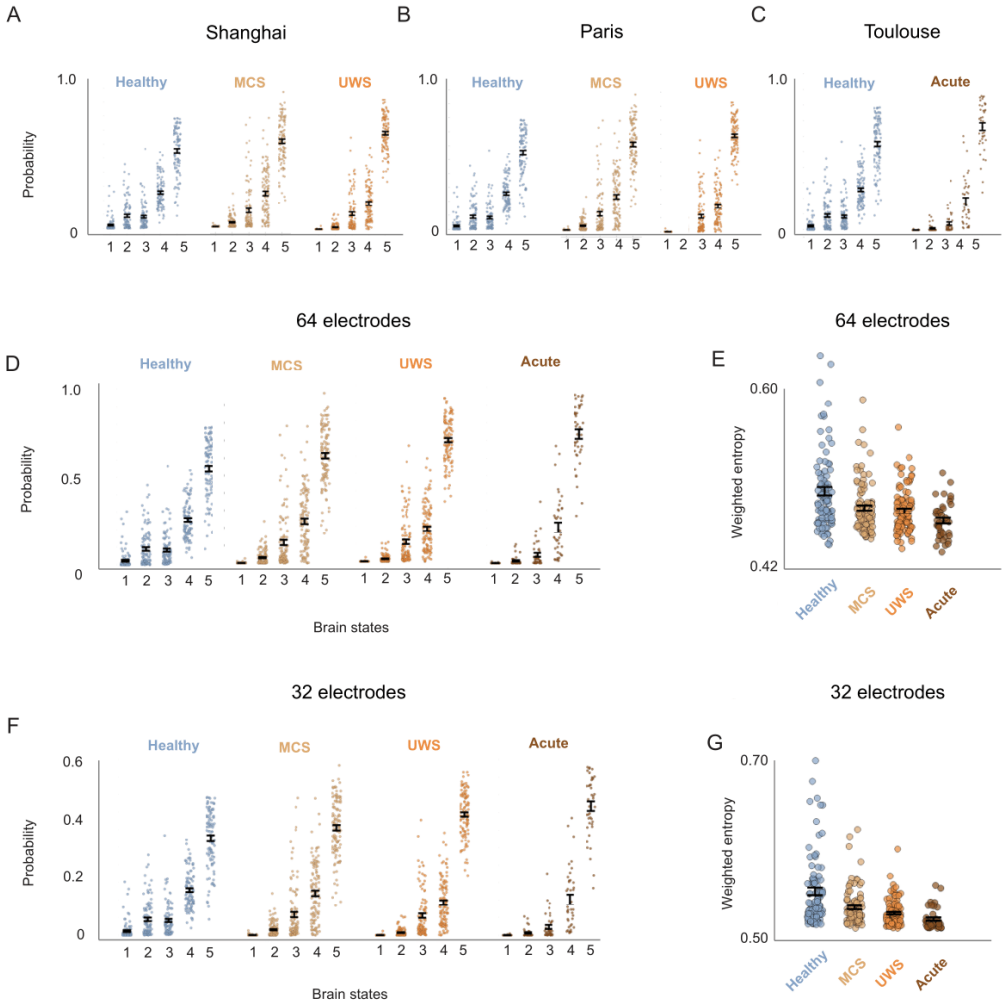

Supplementary Figure 4. Consistency of Brain States Across Datasets and Electrode Number. A-C) Brain states ordered by entropy from 1 (high entropy) to 5 (low entropy), calculated independently for all centers. The brain states display a consistent pattern across datasets, with high-entropy states associated with healthy subjects and the frequency of low-entropy states correlating with the severity of the condition in patients. D) Probability distribution obtained with 64 electrodes. E) WE obtained with 64 electrodes. F) Probability distribution obtained with 32 electrodes. G) WE obtained with 32 electrodes.

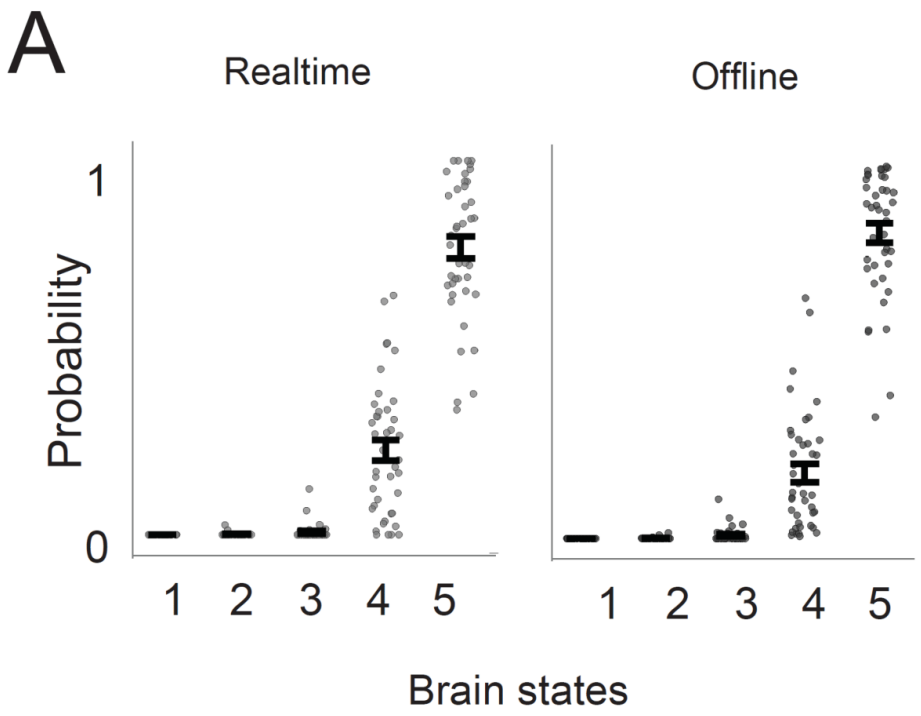

883

884 **Supplementary Figure 5. Real time and offline acute-patient brain state**
885 **distributions.** Comparison of brain state distributions in acute patients obtained through
886 real-time and offline EEG analyses. This figure illustrates the consistency between real-
887 time estimations and offline calculations, highlighting the reliability of real-time EEG-based
888 brain state assessments.

889

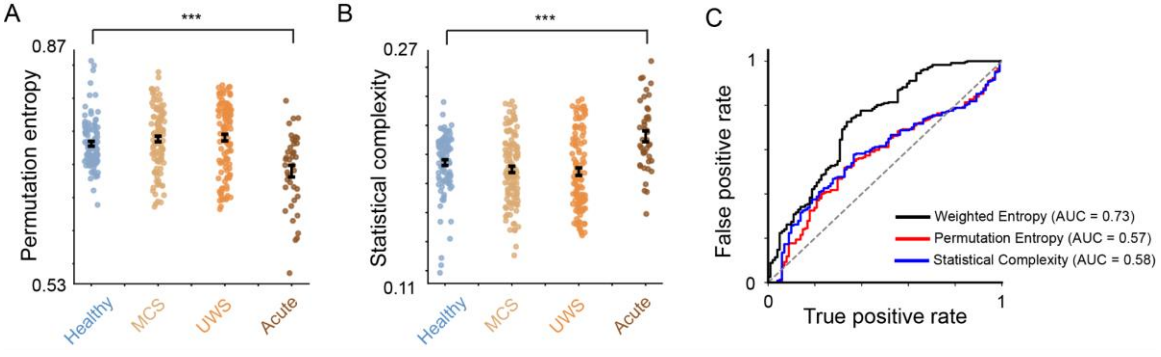

890

Supplementary Figure 6. Entropy and Complexity of the Timeseries. A) Shannon entropy of the timeseries across conditions. Entropy is lower in Acute compared to the other conditions, with a statistically significant difference relative to Healthy (***p < 0.001). B) Statistical complexity of the timeseries for each condition. Complexity is higher in Acute compared to the other conditions, with a statistically significant difference relative to Healthy (***p < 0.001). C) ROC curves for binary classification using three different features: weighted entropy (black), permutation entropy (red), and statistical complexity (blue). The ROC curve corresponding to weighted entropy demonstrates superior performance, with a higher true positive rate across most false positive rates, indicating better discriminative power compared to the other two features.

Supplementary Table 1. Age and gender for all participants.

Supplementary Table 2. Correlation between brain states obtained from different experimental conditions. Participants listened to words, phrases and sentences while EEG was recorded.

Supplementary Table 3. Summary of preprocessing parameters for the three sites.